

K*-shell electron shake-off accompanying alpha decay

M. S. Rapaport, F. Asaro, and I. Perlman†

Lawrence Berkeley Laboratory, University of California, Berkeley, California 94720

(Received 22 July 1974)

The α spectra associated with *K*-shell electron shake-off in ^{210}Po and ^{238}Pu decay have been determined by *K* x-ray- α coincidence measurements. Although the shapes of the spectra generally agree with the theoretical expectations, some discrepancies are observed. The abundances per α particle of the total *K* electron shake-off effect were also determined in these measurements and found to be $(1.65 \pm 0.16) \times 10^{-6}$ for ^{210}Po and $(0.83 \pm 0.11) \times 10^{-6}$ for ^{238}Pu . These results are also compared with theoretical predictions and further experimental and theoretical studies are suggested.

[RADIOACTIVITY ^{238}Pu , ^{210}Po ; measured α -*k* x-ray coin. Deduced electron shake-off abundances, energy distributions. Hartree-Fock-Slater treatment.]

I. INTRODUCTION

The phenomenon by which an electron in a given orbital is excited into the continuum (shake-off) during nuclear decay was first treated by Migdal¹ and Feinberg² and later by Levinger.³ Since then much theoretical⁴⁻⁷ and experimental⁸⁻¹² work related to β^- , β^+ , and electron capture (EC) decay has been done. The various experimental works involved measurements of x-ray- β coincidences, β and x-ray intensities, relative x-ray and γ -ray intensities, and relative intensities of x rays in parent and daughter nuclei. Shake-off of *L* electrons accompanying internal conversion in the *K* shell was also observed.¹³ The agreement between theory and experiment has in general been good.

Essentially, all of the measurements¹⁴ of electron shake-off during α decay have been made on ^{210}Po with one unpublished result on ^{238}Pu . In the ^{210}Po experiments the x-ray abundances were measured and any excess over that expected from the internal conversion of the 803 keV γ -ray was assumed to be due to electron shake-off. The measurement¹⁵ of the *K*-shell effect in ^{238}Pu decay was very similar, but more involved because of additional γ rays. The agreement between experiment and theory has not been good. Generally, the experimental results for the *K*-shell probability were about 60% of the theoretical predictions, and the discrepancy was about twice the stated experimental error.

An electron ejected by the passage of an α particle through the Coulomb field shares in a complementary fashion in the α emission energy. The α spectrum associated with electron shake-off from a particular subshell will have a maximum

energy equal to essentially the α particle energy without shake-off less the binding energy of the electron. The present work was undertaken to measure directly that part of the α spectrum connected with the electron shake-off effect in the *K* shell and to determine the differential shape of this spectrum and compare it with theoretical predictions. We hoped to improve the precision of previous measurements of the total *K* shell probability and delineate more clearly the discrepancy between experiment and the Migdal theory.

II. EXPERIMENTAL WORK

A. Equipment

The general experimental procedure was to measure the α spectra of ^{210}Po and ^{238}Pu which were in coincidence with *K* x rays.

1. *K* x-ray side

The *K* x rays were detected with a solid state detector of pure Ge which has a full-width at half-maximum (FWHM) of 1.0 keV for a 122 keV γ ray and an over-all detection efficiency of 13.5% at that energy.

The output was amplified and fed into a single channel analyzer. In the ^{210}Po measurement this analyzer was set on the K_{α} x rays, which comprise 78%¹⁶ of the total. In the ^{238}Pu measurement, however, the single channel analyzer was set on the K_{β} x rays (~111 keV), which are only 23%¹⁶ of the total *K* x rays, in order to eliminate the α spectrum in coincidence with the 99.8 keV γ ray ($K_{\alpha 2}$ energy = 98.4 keV). In this latter experiment the γ -ray output of the preamplifier was gain-stabilized. The output of the single channel ana-

lyzer was part of a fast-slow triple coincidence system. The block diagram is shown in Fig. 1.

2. α side

The α particles were detected with Au-Si surface-barrier type detectors with geometries of about 2–3%. The intense bombardment of the detector by the α activity of the sources resulted in a deterioration of resolution over the course of the experiments. In the ^{210}Po measurement the FWHM changed from 22.5 keV at the beginning of the experiment to 30.0 keV at the end. For the ^{238}Pu measurement the FWHM changed from 30.0 to 36.5 keV.

The α detector output was first sent to a gain-stabilizer. Then part of the output was fed into the triple coincidence system, part was fed into a unit which scaled down the counting rate by a factor of 20, and part was fed to a 400 channel pulse height analyzer through a bias amplifier and a linear gate. The linear gate was triggered via a mixer gate by either pulses from the triple coincidence system or the scaled-down α singles pulses. The pulse height analyzer was also gated by the triple coincidence system via the gain-stabilizer so that only coincidence pulses were stored and not the scaled-down singles used for gain stabilization.

The net effect of the electronic arrangement was

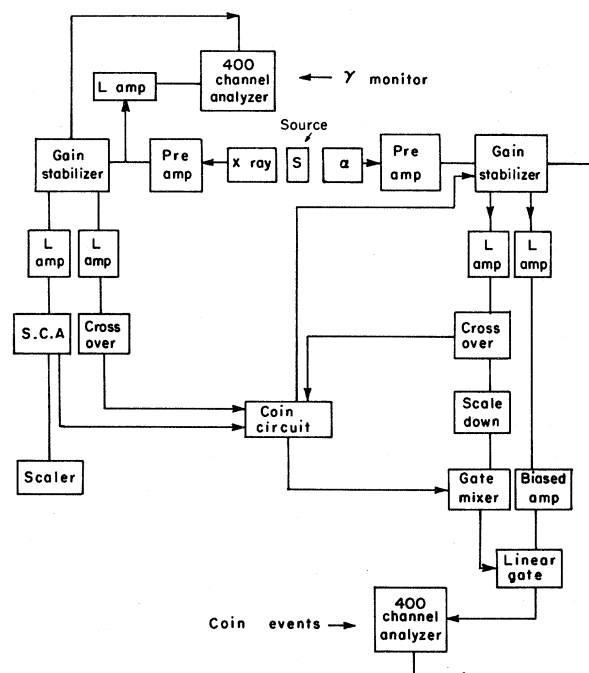


FIG. 1. Block diagram of electronics used for α -x-ray coincidence measurements.

that α pulses which were in coincidence with the K x-ray gate could register on the pulse height analyzer with a minimum of accidental coincidences (72×10^{-9} sec resolving time) and without any gain change during the experiment.

B. Source preparation

The ^{238}Pu was chemically purified by dissolving in 12 M HCl, loading onto an anion column (DOWEX AG 1 \times 8%), washing the column with 12 M HCl containing some HNO_3 , and eluting the ^{238}Pu off the column with a solution 12 M in HCl and 0.44 M in HI. The eluent was evaporated to dryness and then vaporized in vacuum from a tungsten filament onto a 0.05 mm thick mylar foil. The source which had been collimated to an area 8 mm in diameter during vaporization was invisible and had an activity of $\sim 1.2 \times 10^7$ α dis/min.

Two vials of ^{210}Po were purchased from New England Nuclear. The ^{210}Po was catalogued as carrier-free and of natural origin, although investigation at the conclusion of the experiment showed it was prepared by the reaction and decay $^{209}\text{Bi}(n, \gamma)^{210}\text{Bi} \xrightarrow[5 \text{ day}]{\beta^-} ^{210}\text{Po}$. The ^{210}Po from one of the vials was further purified by fuming to near dryness with concentrated HNO_3 , loading onto a cation column (DOWEX 50) with 0.2 M HCl, washing with 2 M HNO_3 , and eluting the ^{210}Po with 2 M HCl. The eluent was evaporated to dryness and vaporized like the ^{238}Pu onto a 0.05 mm thick Mylar foil. The source was $\sim 1.7 \times 10^7$ α dis/min and was invisible.

C. Results

1. ^{238}Pu

The ^{238}Pu was measured in the coincidence unit for a total running time of 15 days. The α singles spectra were measured and recorded every day, as were the coincident spectra. The γ singles spectra were monitored continuously. The α - K

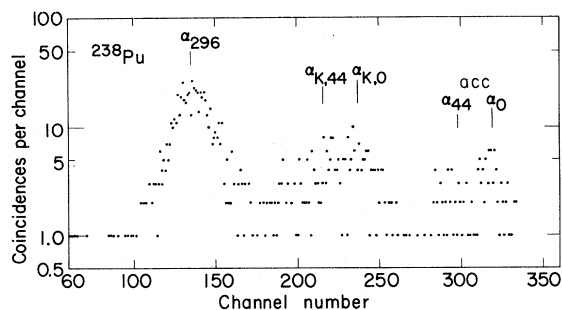


FIG. 2. ^{238}Pu α spectrum in coincidence with uranium K_{β} x rays.

x-ray coincidence spectra for the one day runs were summed and this total spectrum is presented in Fig. 2. The abscissa is the analyzer channel in which the coincidences appeared, and it is roughly linear with the α particle energy. The ordinate is the total number of observed coincidences in the 15 day period. The highest energy peaks, α_0 and α_{44} , are due to accidental coincidences between the most intense α groups and radiation in the K x-ray gate. The most intense peak, α_{296} , is due to true coincidences with K x rays from conversion of the 153 keV γ ray and with the Compton background of this γ ray in the K x-ray gate region. The pertinent part of the ^{238}Pu decay scheme is shown in Fig. 3.

The α_{296} coincident peak (Fig. 2) is broader than the α_0 and α_{44} accidental peaks and this is probably due to a combination of effects including shifts in the threshold of the bias amplifier and a nonlinearity in the pulse height analyzer. The broad α distribution (Fig. 2) in the region of channels 175–260 is broader than α_{296} , tails substantially more on the low energy side and, if we exclude the shake-off effect, would not correspond to any α groups of ^{238}Pu expected to be in coincidence with the K_{β} x ray gate. A measurement was made of the maximum amount of the 100 keV γ ray of ^{238}Pu which could be in the gate region. It indicated that only a negligible proportion of the coincidences in the region of channels 175–260 could be due to this γ ray. To determine if these observed coincidences had the proper maximum energy for a ^{238}Pu α_0 particle which ejected a K electron with about zero kinetic energy we extrapolated their high energy side (Fig. 2) and that of ^{238}Pu α_0 to $\sim\frac{1}{4}$ of their peak height. There was a difference

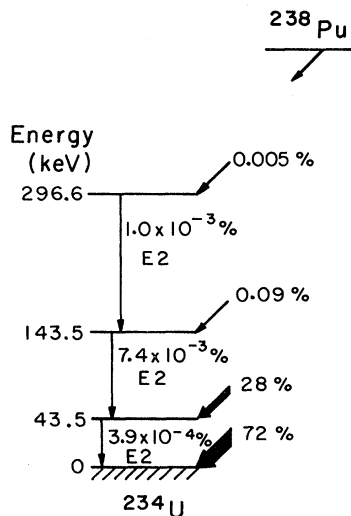


FIG. 3. Partial decay scheme of ^{238}Pu .

in energy of 115 ± 10 keV which agrees with the K binding energy of uranium, 115.6 keV.

Thus, the distribution in Fig. 2 in the region of channels 175–260 should be due to the electron shake-off effect of the main α groups. The distribution is spread out over so many channels because there are two major α groups involved, α_0 and α_{44} , and because the shake-off electrons carry off energy, causing a spread in α particle energy and a tailing on the low energy side. There was a total of 271 coincidences (~ 264 true and ~ 7 accidentals) measured in the 15 day experiment in the region of interest (channels 175–260). From the true coincidence counting rate, the α singles counting rate, the K x-ray side detector efficiency (including geometry), the fraction of total K x rays in the gate and the K shell fluorescence yield, the abundance of ejected K shell electrons is $(0.83 \pm 0.11) \times 10^{-6}$ per ^{238}Pu α particle. This value includes an estimated 10% contribution of undetected coincidences below channel 175. This estimate assumes the same energy dependence as found for the ^{210}Po spectrum which is discussed in the next section.

The nomenclature for the normal α groups shown in Fig. 2 is the usual one with the energy of the excited state being a subscript to the α symbol, e.g., the ^{238}Pu α groups populating the 44 keV excited state in ^{234}U is designated ^{238}Pu α_{44} , or simply α_{44} . We suggest for the α groups ejecting orbital electrons in their passage through the Coulomb field, that the shell designation of the ejected electrons be added as a subscript before the excited state energy. Thus, the ^{238}Pu α group which populates the 44 keV state in ^{234}U and which also causes a K electron to be ejected would be designated ^{238}Pu $\alpha_{K,44}$, or simply $\alpha_{K,44}$.

2. ^{210}Po

The ^{210}Po was also measured in the coincidence unit for a total running time of 15 days. The ex-

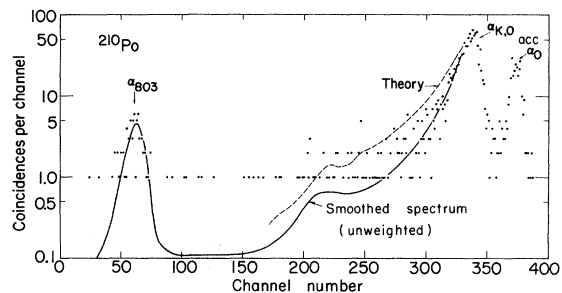


FIG. 4. ^{210}Po α spectrum in coincidence with lead K_{α} x rays. --- shows theoretical shape normalized to peak height.

periment was very similar to that for ^{238}Pu except that a larger fraction of the K x-ray peak could be used in the gate as there are no γ rays in ^{210}Po decay near the gate energy. The various coincidence runs in the 15 day period were summed and the total spectrum is shown in Fig. 4. The highest energy peak α_0 is due to accidental coincidences with the main α group. The only other known α group of ^{210}Po populates the 803 keV excited state of ^{206}Pb and has a very low abundance¹⁷ of 1.07×10^{-5} . The peak at \sim channel 340 (Fig. 4) is broader than α_0 and tails more on the low energy side.

The linearity of the amplifier-analyzer system for α particles was carefully checked with ^{240}Pu and ^{242}Pu and was found to be linear within 1% in the region of interest. Thus, the increased peak width is not due to nonlinearity in the energy scale and is very likely caused by the kinetic energy carried off by the K electrons ejected during the α decay process, as in ^{238}Pu decay. By extrapolating the two peaks (Fig. 4) in the same fashion as for the ^{238}Pu experiment, we found the difference in energy was 88 ± 1 keV, in excellent agreement with the K shell binding energy of lead, 88.0 keV.

There was a total of 1347 coincidences (\sim 1285 true and \sim 62 accidental) in the region of the α shake-off peak, ^{210}Po $\alpha_{K,0}$. Calculated in the same way as for the ^{238}Pu experiment, the abundance of ejected K shell electrons is $(1.65 \pm 0.16) \times 10^{-6}$ per ^{210}Po α particle. As a check on the correctness of our geometry calibration, we calculated the K conversion coefficient of α_{803} from its abundance in the coincidence run (Fig. 4) and the tabulated singles abundance, 1.07×10^{-5} . The resulting value $(8.1 \pm 1.4) \times 10^{-3}$ is in good agreement with the theoretical¹⁸ $E_2 K$ conversion coefficient, 8.08×10^{-3} .

III. DISCUSSION

Migdal treated the α decay shake-off phenomenon as an example of an adiabatic perturbation since the velocities of the α particles are much smaller than the velocities of the inner electrons. As indicated earlier, his calculations for the K shell give results about a factor of 2 higher than the experimental values. Lvinger modified Migdal's treatment by including the recoiling nucleus in the perturbation which reduced the probability of the shake-off taking place by about an order of magnitude. There has been considerable controversy on the magnitude of the recoil effect, with several authors¹⁹⁻²² indicating it was significant. Two papers^{23,24} suggest the recoil effect is negligible, with the treatment in the former being qual-

itative and that in the latter probably containing errors in the calculation of the recoil kinetic energy. In addition, Ciocchetti and Molinari²² predicted an electron monopole contribution which was substantially larger than the dipole contribution, which is all that is normally calculated with the Migdal theory for the K shell. The present theoretical work does not enter into these controversies but attempts to determine for the Migdal treatment if Hartree-Fock-Slater (HFS) instead of hydrogenic wave functions improve the agreement with experiment.

According to Migdal theory the differential probability of ionizing one of the electrons may be expressed as

$$dP_{1s} = \frac{8v^2}{3(E_K - B)^4} |\langle k, l = 1 | \frac{1}{r^2} | 1s \rangle|^2 dE_k + \text{smaller terms}, \quad (1)$$

where v is the velocity of the α particle, r is the radial distance from the nucleus, B is the binding energy of a $1s$ electron, l is the angular momentum of the continuum states, E_k is the kinetic energy carried off by the ionized $1s$ electron, and $k = (2E_k)^{1/2}$. This equation is like Migdal's equation (15) except the summations over the angular part of the wave function and of the two electrons have been carried out. The matrix element can be readily calculated with hydrogenic wave functions and the probability equation becomes

$$dP_{1s} = \frac{2^{11}v^2}{3Z^6} \frac{e^{-(4Z/k) \arctan(k/Z)}}{(1 + k^2/Z^2)^5 (1 - e^{-2\pi Z/k})} dE_k, \quad (2)$$

where Z is the charge of the daughter nucleus. One gets the total ionization probability by numerical integration. Equation (2) differs from Migdal's equation (19) by a sign misprint in the k^2/Z^2 term and also by a factor of $1/(2Z^2)$. This may be due to the way in which Migdal normalized his continuum wave function. He may have used the same factor, $2n^3/[1 - e^{-\pi Z(2/E)^{1/2}}]$, as in his β decay treatment. The factor of 2 is already included for α decay in Migdal's equation (18) and the normalization factor should be divided by Z^2 . This is in addition to the $1/Z^2$ factor in Migdal's equation (16) and the $1/Z^2$ factor used for the matrix elements of discrete states shown after Eq. (18). Migdal's equations (9)-(11) and (20)-(22) and the values in his Tables 1 and 2 do not depend on this normalization and would therefore not be in error from this effect.

A more realistic set of wave functions would be of the self-consistent type. We used the tabulated²⁵ Hartree-Fock-Slater central potentials to solve the Schrödinger equation for the continuum electrons and applied the Noumerov integration meth-

TABLE I. Probability of electron shake-off from the K shell.

Isotope	Ref.	Experiment	Stated error	Theory (hydrogenic)	Theory (HFS)
^{210}Po	29	1.5×10^{-6}	$\pm 33\%$		
	30	2.0×10^{-6}	$\pm 16\%$		
	31	1.6×10^{-6}	$\pm 31\%$		
	23	1.5×10^{-6}	$\pm 27\%$		
	This work	1.65×10^{-6}	$\pm 10\%$	2.67×10^{-6}	2.87×10^{-6}
^{238}Pu	15	0.51×10^{-6}	$\pm 50\%$		
	This work	0.83×10^{-6}	$\pm 13\%$	1.75×10^{-6}	1.66×10^{-6}

od.²⁶ The two points at small r required to generate the solutions were taken to be hydrogenic. The asymptotic solution is known to be²⁷

$$P_{kl}(r) = R_w r \approx (2/\pi k)^{1/2} \cos[kr + k^{-1} \ln(2kr) - \frac{1}{2}\pi(l+1) - \delta_l], \quad (3)$$

where R_w is the radial wave function normalized in the energy scale, l is the orbital angular momentum quantum number, and $\delta_l = \arg \Gamma(l+1+iz/k)$ is the complex phase of the Γ function. Using the derivative of (3) we can write

$$P_{kl}^{\prime 2}(r) + \frac{P_{kl}^{\prime 2}(r)}{(k+1/kr)^2} = \frac{2}{\pi k}. \quad (4)$$

Equation (4) is independent of r for large r . Thus, the numerical solution for the continuum wave functions can be normalized by requiring Eq. (4) to hold for large r . With these solutions and the tabulated²⁵ $1s$ wave functions we calculated²⁸ the matrix elements in Eq. (1) and obtained the probability vs energy relation. The total probability was obtained by numerical integration. Table I summarizes the experimental results and our theoretical results on the shake-off effect in α decay.

Using our calculations of shake-off probability as a function of electron energy and the experimental average peak shape in the ^{210}Po α singles spectrum, we determined the shape of the α spectrum associated with the shake-off of K electrons which would be expected from Migdal's theory. The theoretical shape was normalized to the same peak height as the experimental curve and is shown as a dashed line in Fig. 4. The α singles spectrum had a small perturbation about 300 keV below the peak due to instrumental effects and this is reflected in both the calculations and the coincidence spectrum. As seen in Fig. 4, there is a definite discrepancy between the experimental and theoretical curves. The probability of electron shake-off

decreases more rapidly than the theoretical prediction as the electron energy increases (i.e., as the α particle energy decreases). Ovechkin and Tsenter²³ observed the same effect in comparing electron energy measurements with Migdal's calculations, but the authors felt their experimental work was not sufficiently precise to indicate a definite discrepancy.

A distinctly different type of theoretical treatment was published recently by Hansen²⁴ after the present work was concluded. Hansen obtained a value of 2.02×10^{-6} for the total K shell ionization probability for ^{210}Po , which is somewhat closer in agreement with the experimental result than any of the theoretical values. Although not discussed in the present work, Hansen's calculations for L and M shells were in far better agreement with the experimental results than any other theory.

IV. SUMMARY AND SUGGESTIONS

It is clear that Migdal's theory still predicts ionization probabilities approximately twice as high as observed experimentally. The use of HFS type wave functions has little effect on the total ionization probabilities. Also, the energy distributions calculated with HFS type wave functions are almost identical with those calculated with the hydrogenic type. The theoretical energy distribution of the ejected electrons does not fall off as rapidly with increasing energy as the experimental one.

It is possible the discrepancies mentioned above could be reduced by using relativistic Hartree-Fock wave functions. These wave functions should be made very accurate at small distances, since this is the region where most of the strength of the matrix elements lies.

An experimental study of ^{148}Gd similar to the ones presented in this paper should indicate if Migdal's theory gives the proper dependence on both charge and α particle energy. Very large discrepancies exist between Migdal's theory and

experimental shake-off measurements for the L and M shells. More precise measurements in which the abundance (L , M , and N subshells) and electron energy dependence (L subshells) are determined for each subshell could help indicate the sources of these discrepancies. Measurements of the abundance of N shell effect, which should be substantially larger than that in the M shell, could indicate what would be the "best" α

peak shape or resolution which present-day high-resolution α spectrometers could obtain.

After the manuscript was submitted a similar paper was published by Briand *et al.*³²

We are very grateful to Duane Mosier of the Lawrence Berkeley Laboratory for many consultations and detailed suggestions on the types of equipment used in these experiments.

*Work performed under the auspices of the U. S. Atomic Energy Commission.

†Present address: The Hebrew University, Jerusalem, Israel.

¹A. Migdal, *J. Phys. USSR* **4**, 449 (1941).

²E. L. Feinberg, *J. Phys. USSR* **4**, 423 (1941).

³J. S. Levinger, *Phys. Rev.* **90**, 11 (1953); *J. Phys. Radium* **16**, 556 (1955).

⁴T. A. Carlson, C. W. Nestor, Jr., T. C. Tucker, and F. B. Malik, *Phys. Rev.* **169**, 27 (1968).

⁵A. J. Mord, *Nucl. Phys.* **A192**, 305 (1972).

⁶J. Law and J. L. Campbell, *Nucl. Phys.* **A185**, 529 (1971); *Nucl. Phys.* **A187**, 525 (1972); *Nucl. Phys.* **A199**, 481 (1973).

⁷T. Mukoyama, Y. Isozumi, T. Kitahara, and S. Shimizu, *Phys. Rev. C* **8**, 1308 (1973).

⁸C. W. E. Van Eijk and R. W. Kooy, *Phys. Lett.* **46B**, 351 (1973).

⁹J. L. Campbell and J. Law, *Can. J. Phys.* **50**, 2451 (1972).

¹⁰Y. Isozumi and S. Shimizu, *Phys. Rev. C* **4**, 522 (1971).

¹¹E. der Mateosian, *Phys. Rev. A* **3**, 573 (1971).

¹²H. J. Nagy, G. Schupp, and R. R. Hurst, *Phys. Rev. C* **6**, 607 (1972).

¹³F. T. Porter, M. S. Freedman, and F. Wagner, Jr., *Phys. Rev. C* **3**, 2246 (1971).

¹⁴W. Rubinson, *Phys. Rev.* **130**, 2011 (1963).

¹⁵C. M. Lederer, private communication.

¹⁶G. C. Nestor, B. G. Saunders, and S. T. Salem, *At. Data* **1**, 377 (1970).

¹⁷*Nucl. Data* **B5/6**, 648 (1971).

¹⁸R. S. Hager and E. C. Seltzer, *Nucl. Data* **A4**, 1 (1968).

¹⁹H. M. Schwartz, *Phys. Rev.* **100**, 135 (1955).

²⁰F. Grard, *C. R. Acad. Sci. (Paris)* **243**, 777 (1956).

²¹W. Rubinson, *Phys. Rev.* **130**, 2011 (1963).

²²G. Ciocchetti and A. Molinari, *Nuovo Cimento* **40B**, 69 (1965).

²³V. V. Ovechkin and E. M. Tsenter, *At. Energ. (USSR)* **2**, 282 (1957) [*Sov. J. At. Energy* **2**, 344 (1957)].

²⁴J. S. Hansen, *Phys. Rev. A* **9**, 40 (1974).

²⁵F. Herman and S. Skillman, *Atomic Structure Calculations* (Prentice-Hall, Englewood Cliffs, N. J., 1963).

²⁶J. M. Blatt, *J. Comput. Phys.* **1**, 382 (1967).

²⁷H. Bethe and E. E. Salpeter, *Quantum Mechanics of One and Two Electron Atoms* (Academic, New York, 1957), p. 23.

²⁸M. S. Rapaport, Ph.D. thesis, University of California, LBL Report No. LBL-2978, 1974 (unpublished).

²⁹M. A. Grace, R. A. Allen, D. West, and H. Halban, *Proc. Phys. Soc. Lond.* **A64**, 493 (1951).

³⁰W. C. Barber and R. H. Helm, *Phys. Rev.* **86**, 275 (1952).

³¹M. Riou, *J. Phys. Radium* **13**, 487 (1952).

³²J. P. Briand, P. Chevallier, A. Johnson, J. P. Rozet, M. Tavernier, and A. Touati, *Phys. Rev. Lett.* **33**, 266 (1974).